

## **Outside fortified solid pillar section joint exposed to monotonic stacking**

Sudeepta Kishor Dash, Sattwik Mallik, Amlan Pattnayak, Shradha Jena

*Department of Civil Engineering, NM Institute of Engineering and Technology, Bhubaneswar, Odisha*

*Department of Civil Engineering, Raajdhani Engineering College, Bhubaneswar, Odisha*

*Department of Civil Engineering, Aryan Institute of Engineering and Technology Bhubaneswar, Odisha*

*Department of Civil Engineering, Capital Engineering College, Bhubaneswar, Odisha*

---

**ABSTRACT:** The joints among pillars and segments are vital zones in a strengthened solid second opposing edge. The conduct of such joints incredibly impacts the strength and pliability of the general edge. In this examination, investigation of three-dimensional mathematical models of outside fortified solid bar section joints under monotonic stacking was performed utilizing the limited component ABAQUS bundle. Concrete and strengthening steel material nonlinearities, just as bond qualities between fortifying bars and encompassing cement were considered in the investigation. A parametric report including thirty joint models was led to look at the impact of con-crete strength, section pivotal burden, joint stirrups and state of the shaft top fortification on the pillar tip burden and relocation limits. The solid measurements and fortification of the stud-ied models were picked to guarantee the event of joint disappointment. The investigation indicated that the shaft tip extreme burden fundamentally expanded as the solid strength, segment hub burden and joint mix rups were expanded. Joints with L-molded pillar top fortifying bars showed comparable execution to those with U-formed bars. The utilization of straight bars for bar top support fundamentally decreased the bar tip.

**KEYWORDS:** Reinforced concrete; Beam-column joint; Finite element; Monotonic loading; Numerical analysis; Bond simulation

---

### **I. INTRODUCTION**

The recent laboratory experiments indicated that unsatisfactory structural performance may result from the premature failure of beam-column joints as described by Scott (1992) [1] and by Parker and Bullman (1997) [2]. Therefore, a beam-column joint is a critical zone in reinforced concrete frames which should be designed to provide the sufficient ultimate strength and deformation capacity. Joints around the external border of a structure are more vulnerable to failure than interior joints. The priority in static loading is strength then ductility, therefore, joints in an ordinary structure are designed on the basis of strength to resist gravity and windloads.

There are several possible failure modes that can occur in joints. Such modes include column flexural failure, beam flexural failure, column shear failure, beam shear failure, joint shear failure and bond failure of reinforcement. Numerous numerical studies have been carried out on exterior beam column joints under monotonic loading using different finite element programs. Baglin and Scott (2000) [3] carried out numerical research using SBETA package to simulate exterior beam column joints subjected to monotonic loading and column axial load. They made a validation against 19 tests performed by the authors [1,3] and by Hamil (2000) [4]. The validation specimens had varied beam top reinforcement configuration and concrete compressive strength. Additionally, different numbers of column stirrups in the connection zone were considered. The model took into consideration different types of failure mechanisms involving beam failure, joint diagonal shear cracking, and bond slip. They performed a parametric study involving column load value and different arrangement of joint stirrups. The authors concluded that increasing the column load to a value corresponding to an equivalent stress of 20 MPa ( $f_{cu}/3$ ) increased the joint ultimate capacity, while exceeding this value resulted in the opposite.

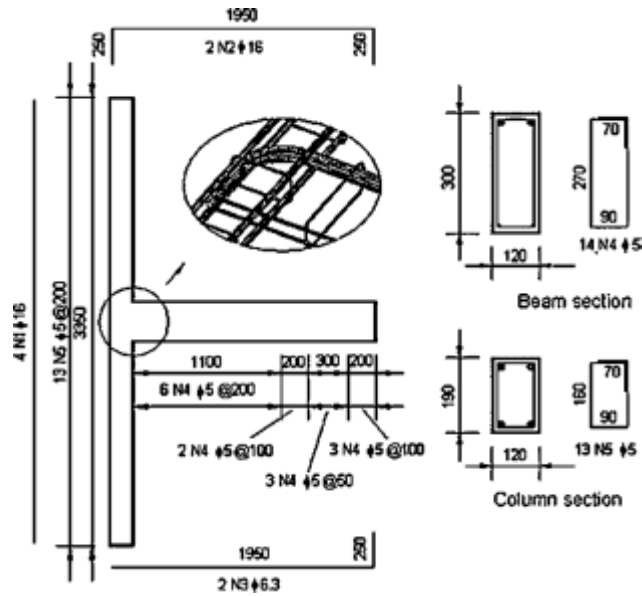


Fig.1 Layout of test specimen, Haachetal. [12].

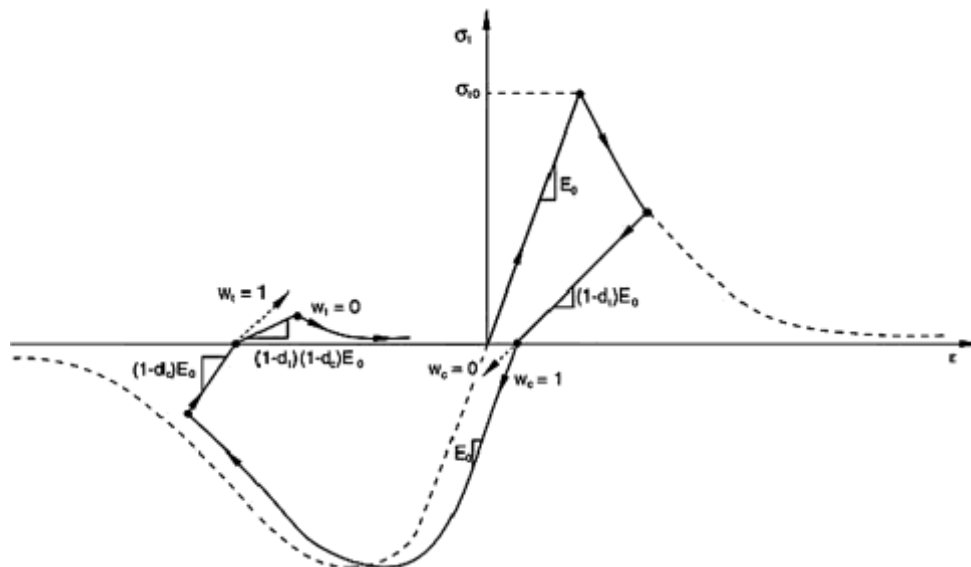


Fig.2 Concrete stress-strain relation with loading and unloading [13].

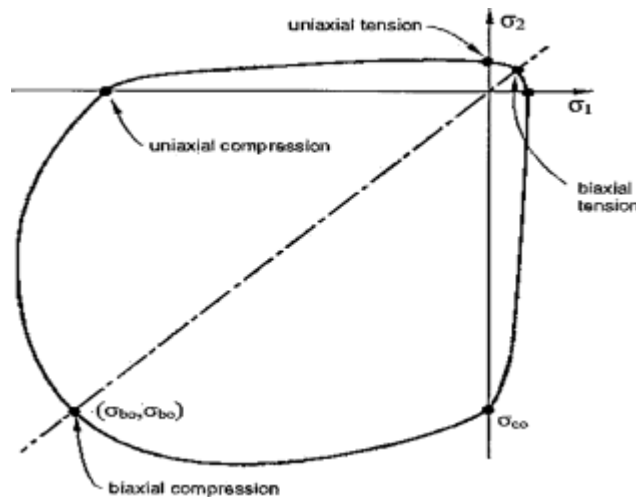
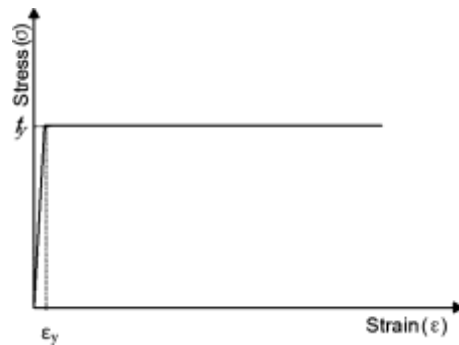


Fig.3 Concrete yield surface in plan stress by Kupfer [13].



**Fig.4 Typical** stress-strain curve for steel reinforcement.

Moreover, the rise of axial load also improved the top beam bars anchorage within the joint as well as the joint stiffness. In addition, the more closely spaced stirrups within the joint increased the joint ultimate capacity by limiting the extension of joint shear cracks as well as improving the contribution of the bent-down bars of the beam by increasing the confinement around them.

Bakir and Boduroglu (2002) [5] suggested a new empirical design equation for exterior joints subjected to monotonic loading based on 58 tests involving a large parametric study such as the beam reinforcement ratios, the stirrups of the joint core, the beam reinforcement detailing (U or L-bars anchorage), and the axial load stress. The authors concluded that increasing the beam reinforcement ratios and joint transverse reinforcement led to increasing shear capacity. In addition, U bar detailing ought not be utilized in monotonically loaded exterior beam column connection. On the other hand, using L bar detailing can change the failure mode from the beam failure to joint shear failure. Furthermore column axial stress had no effect on ultimate joint shear capacity. Atta et al. (2004) [6] carried out finite element analyses using ANSYS to simulate the behavior of beam-column joint subjected to monotonic loading and column axial load. An extensive parametric investigation was performed such as concrete grade, column axial force, girder depth, column dimensions, joint transverse reinforcement, and reinforcement anchorage. The parametric

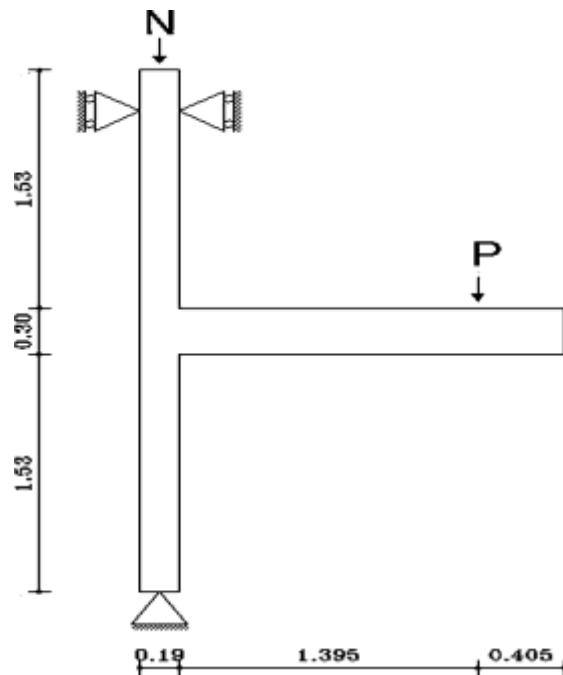


**Fig.5 Loading and boundary conditions (dims in meters).**

study confirmed that the increase of concrete grade increased the ultimate capacity. Moreover, the distribution of joint stirrups had the most noticeable influence in improving the system stiffness and ultimate capacity and a more brittle failure mode was observed due to lesser sharing of joint stirrups. Hegger et al. (2004) [7] discussed the behavior of interior and exterior beam-column joints by using the finite element code ATENA. Two-dimensional plane stress analyses were carried out under monotonic loading only at the beam tip without axial column load. Beam failure and joint compression strut failure were observed. The parameters affecting the shear capacity were different for interior and exterior joints. In case of exterior

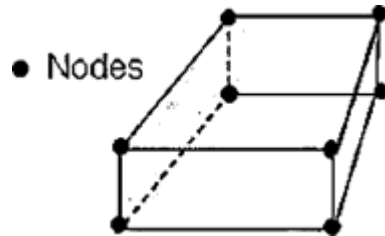


**Fig.6** Typical 8 nodes linear brick element[13].

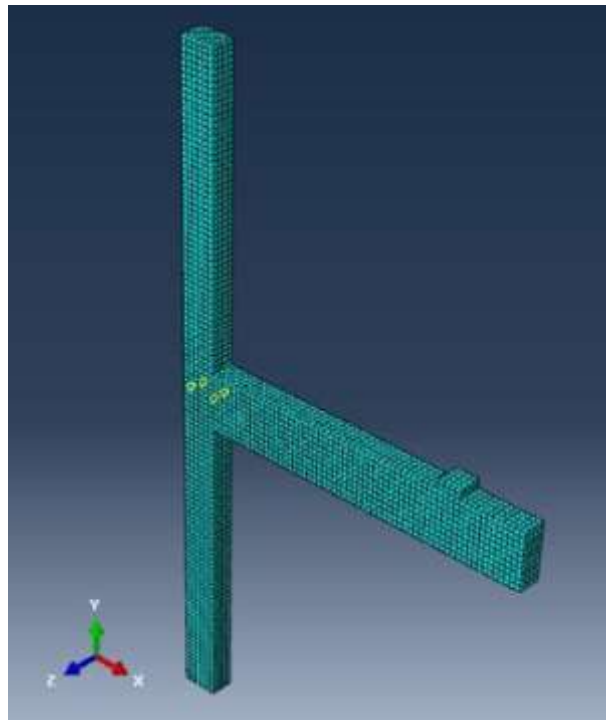


**Fig.7** Numerical model mesh.

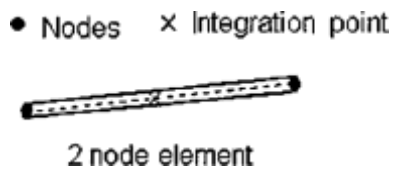


**Fig.8** Typical 2 nodes linear beam element[13].

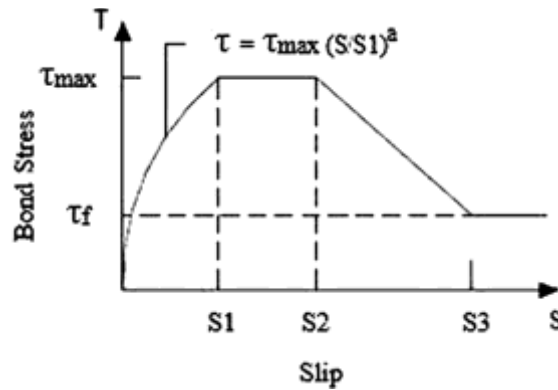


**Fig.9** CEB-FIPMC90 model for bond-slip[14].

beam-column joint, the authors concluded that normal stresses of column higher than 40% of the concrete compressive strength reduce the joint shear strength.

Haach (2005) [8] conducted experimental tests of exterior beam-column joints under monotonic loading and column axial load. The tests contained three specimens with the same characteristics of geometry and material, with different axial load only. The authors used ABAQUS software to perform a numerical simulation. The numerical results were validated against experimental results and revealed good agreement specifically in reinforcement strains. The influence of the axial load level, axial load eccentricity, and joint stirrups ratio were investigated in a parametric study. The specimens collapsed due to shear diagonal cracking. The authors observed that higher column axial load made the joint stiffer and less ductile. Moreover, higher column axial loads generated better bond condition for the beam top reinforcement by increasing the compressive stresses of the anchorage. Patil and Manekari (2013)[9] carried out a numerical research to compare between the behavior of corner and exterior connection subjected to monotonic loading using ANSYS finite element package. Different parameters were analyzed such as maximum principle stress, minimum principle stress, displacement, different boundary conditions, and stiffness variation to make a comparison study. Chaudhari et al. (2014) [10] performed a comparison study between ABAQUS and ANSYS results on exterior beam column joint subjected to monotonic loading. The authors concluded that ABAQUS software gave more realistic findings than ANSYS. Tran and Hadi (2017) [11] conducted an analytical study on exterior beam-column joints subjected to quasi-static cyclic loading. The predicted shear strength of proposed model was compared with five analytical

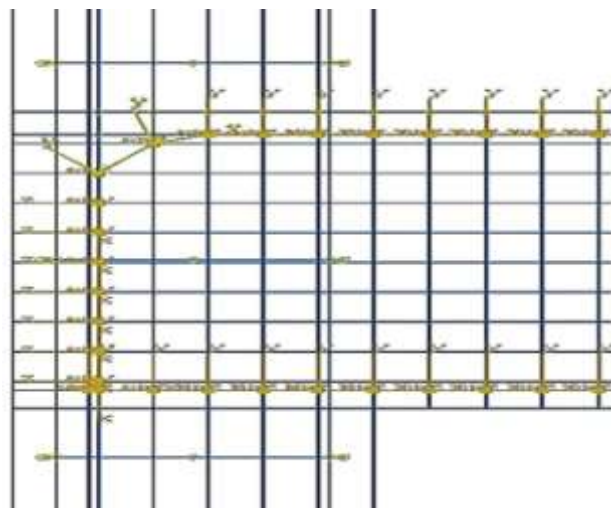


**Fig.10** Beam top bar detail at joint.

models and 142 test results to validate it. Three parameters involving concrete compressive strength, column axial stress level, and the vertical and horizontal amount of shear reinforcement were considered to evaluate the proposed assumption. This assessment revealed that the suggested model can

efficiently anticipate shear strength.

The objective of the present work is to study the effect of axial load ratio, grade of concrete, number of joint stirrups and type of beam top reinforcement anchorage on the strength and deformation capacity of exterior beam-column joints subjected to shear failure. For this purpose, thirty exterior beam-column joints subjected to monotonic loading were numerically

**Table 1** Values of parameters for CEB-FIPMC90 model [14].

	Good bond conditions		All other bond conditions	
	Good bond conditions	All other bond conditions	Good bond conditions	All other bond conditions
S1	0.6mm	0.6mm	1.0mm	1.0mm
S2	0.6mm	0.6mm	3.0mm	3.0mm
S3	1.0	2.5 mm	Clear rib spacing	Clear rib spacing
a	$2.0 \frac{P_{\text{conf}}}{f_{ck}}$	$1.0 \frac{P_{\text{conf}}}{f_{ck}}$	$2.5 \frac{P_{\text{conf}}}{f_{ck}}$	$1.25 \frac{P_{\text{conf}}}{f_{ck}}$
a	0.15	0.15	0.40	0.40

$f_{ck}$ : Characteristic concrete compressive strength

ally modelled and analysed using the finite element program ABAQUS.

## II. NUMERICAL MODELLING BY ABAQUS

### 1.1. Geometry

The considered exterior joint consisted of a beam portion and a column portion similar to the model adopted by Haach et al. [12], Fig. 1. The beam had a cross section of 300 mm x 120 mm with 1800 mm overall length of cantilevered portion. The column had a cross section of 190 mm x 120 mm with a total length of 3350 mm. The beam top reinforcement was 2 bars of 16 mm diameter and bottom reinforcement was 2 bars of 6.3 mm diameter. The beam transverse reinforcement consisted of  $\phi$ 5 mm diameter stirrups spaced at 200 mm as shown in Fig. 1. The column reinforcement was 4 longitudinal bars of 16 mm diameter and 5 mm diameter stirrups spaced at 200mm.

### 1.2. Material model

The concrete damaged plasticity (CDP), which is an adjustment of the Drucker-Prager strength hypothesis, is used in ABAQUS [13] to define concrete material as shown in Fig. 2. The basic constitutive parameters required to determine the CDP material model include: the dilation angle ( $\psi$ ) which is interpreted as the deformation capacity of concrete when subjected to shear stress and is usually taken between  $30^\circ$  and  $40^\circ$ , an intermediate value of  $35^\circ$  was considered in the present study which provided good correlation with available experimental results; the value of flow potential eccentricity ( $m$ ) which was assumed 0.1; the default value of initial biaxial/uniaxial compressive yield stresses ratio ( $r_{bo}/r_{co}$ ) which was taken equal to 1.16 as shown in Fig.3.

An elastic-perfectly plastic stress-strain curve was used to define steel material as indicated in Fig. 4. The yield stress ( $f_y$ ) of beam top reinforcement and column reinforcement was 515 Mpa. The yield stress of beam bottom reinforcement and stirrups was 562.50 Mpa and 684.50 Mpa, respectively.

### 1.3. Loading and boundary conditions

The column was subjected to axial load as a pressure load at the top end according to a pre-specified value which was kept constant during the analysis. Each case was analyzed for a vertical displacement controlled loading that was applied at the end of the beam. The boundary conditions were set in the model as shown in Fig. 5. The column top end was roller, which had a horizontal restricted displacement  $U_x$ . The bottom of the column was hinged which was restrained in two degrees of freedom  $U_x$  and  $U_y$ .

### 1.4. The finite element mesh

Three dimensional Solid 8-nodes brick element with reduced integration scheme (C3D8R) were used to model the concrete in space as shown in Fig. 6. A mesh size of 30 mm was considered for overall elements in concrete part of beam and column as shown in Fig. 7. Three dimensional truss 2-nodes element (T3D2) were used to model the steel reinforcement in space as shown in Fig.8.

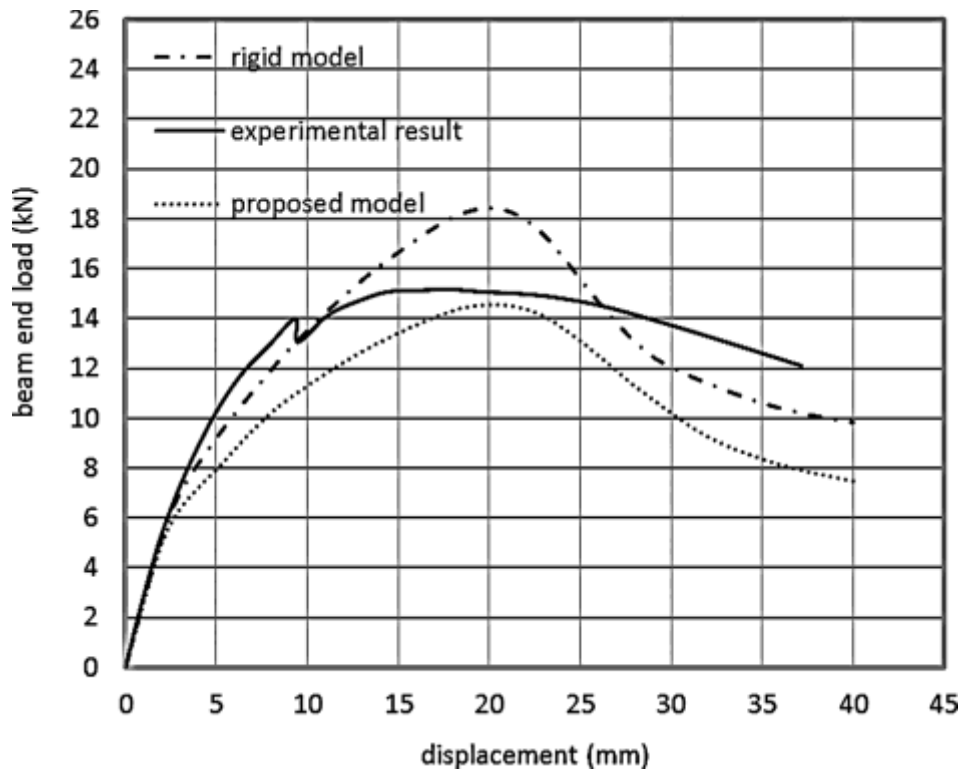


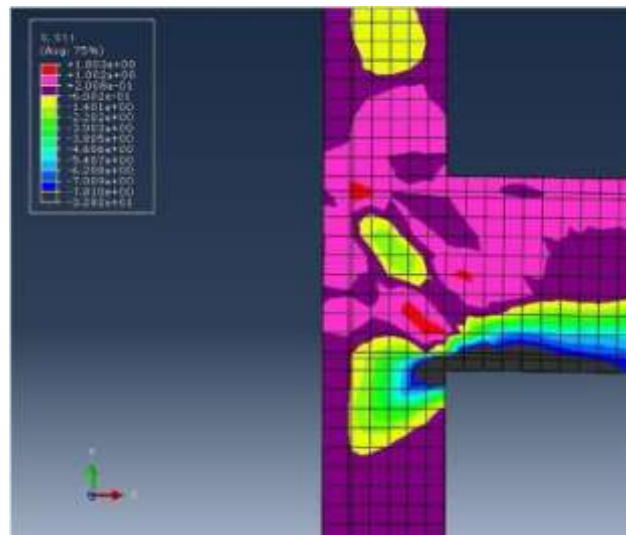
Fig.11 Verification results.

1.5. Connectors

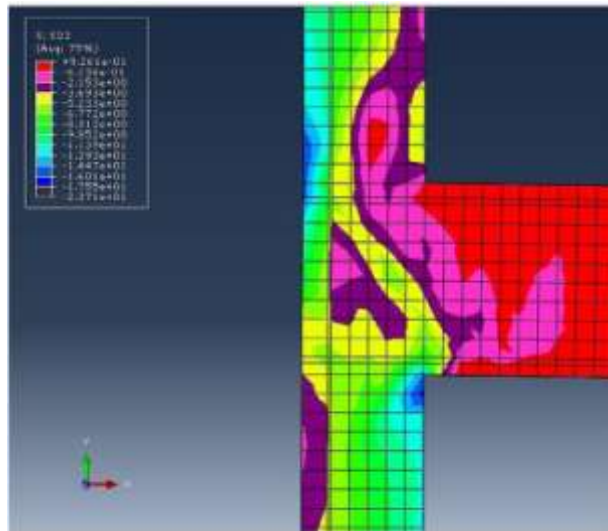
The bond slip between the concrete and steel reinforcement was introduced using connector elements. These connectors modeled the bond strength and the relation between bond stress and relative displacement in the axial direction between the steel reinforcement and the surrounding concrete. The bond law was based on the Euro-International Committee for Concrete (CEB) and the International Federation for Pre-stressing (FIP) Model Code 1990 (CEB-FIPMC90) [14] as shown in Fig. 9 and Table 1. The selected type of concrete used in this model was confined concrete with good bond conditions. Fig. 10 shows the beam top bar detail at joint.

1.6. Verification study

The beam tip load-displacement curve obtained from the numerical analysis using ABAQUS was compared with the reported results from the experimental test which was carried



(a)  $S_{11}$  (X direction)



(b)  $S_{22}$  (Y direction)  
**Fig.12** Concrete stresses.

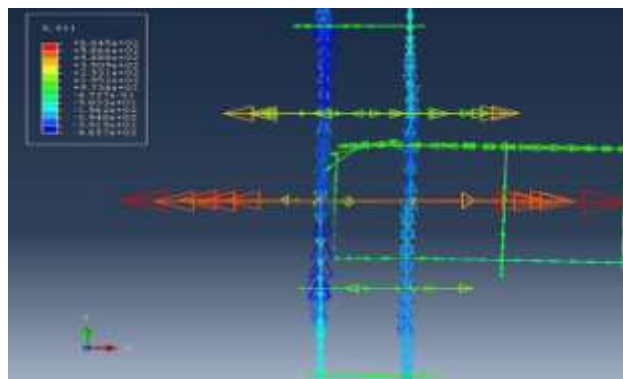
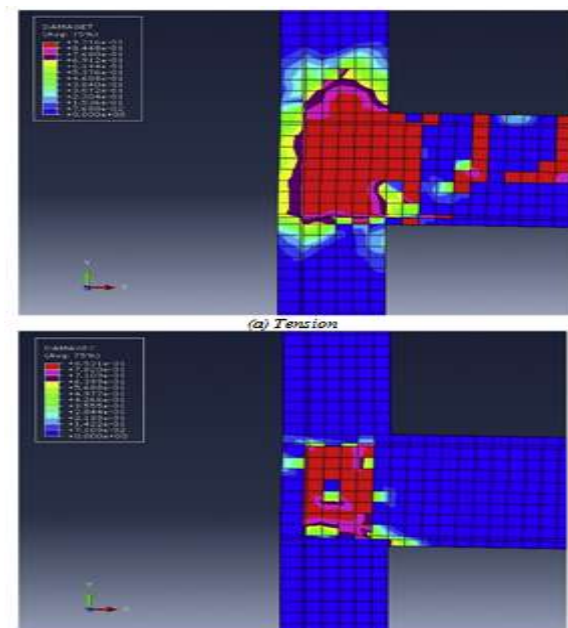


**Fig.13** Reinforcing steel stresses.



(b) Compression  
**Fig.14** Concrete damage.



out by Haach et al. (2014) [12]. To validate the precision of the proposed numerical model, specimen N400 was selected from the experimental database which was the control specimen. The cylinder compressive strength of concrete ( $f_c$ ) was taken equal to 20.53 Mpa. It may be visible that the overall trend of specimen obtained from the numerical simulation is similar

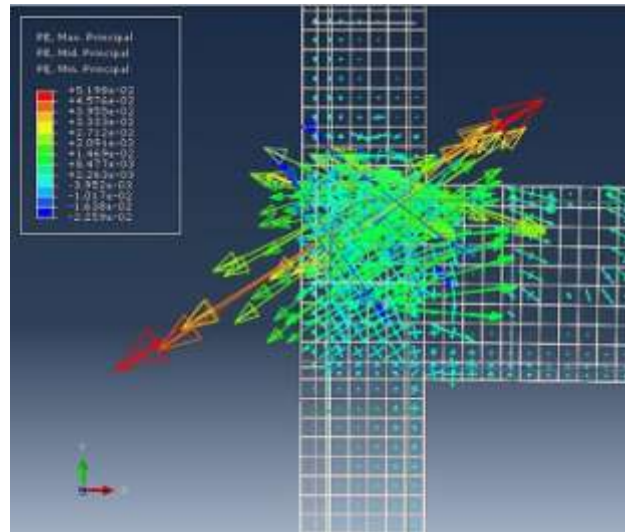


Fig.15 Plastic strain(PE).

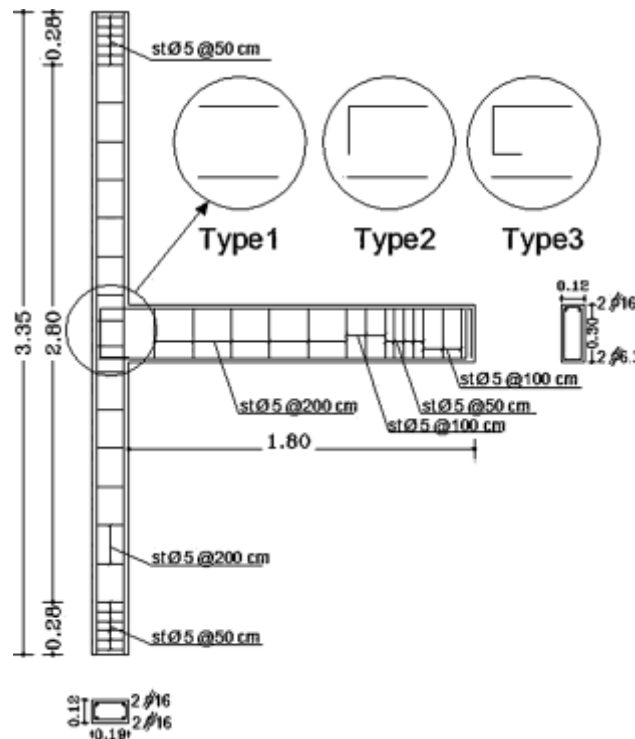


Fig.16 Reinforcement details.

Table 2 Parametric study database.

Joint No.	Compressive Concrete Strength ( $f'_c$ ) Mpa	Axial Load Ratio ( $P/f'_c A_c$ %)	Column stirrups ( $n_s$ )	Type of Anchorage
S1	30	0.3	3	Type 2
S2	40			
S3	50			
S4	30	0	2	Type 1
S5				Type 2
S6				Type 3
S7			3	Type 1
S8				Type 2
S9				Type 3
S10			4	Type 1
S11				Type 2
S12				Type 3
S13		0.3	2	Type 1
S14				Type 2
S15				Type 3
S16			3	Type 1
S17				Type 2
S18				Type 3
S19			4	Type 1
S20				Type 2
S21				Type 3
S22		0.6	2	Type 1
S23				Type 2
S24				Type 3
S25			3	Type 1
S26				Type 2
S27				Type 3
S28			4	Type 1
S29				Type 2
S30				Type 3

to that of the experiment as shown in Fig. 11. In the proposed model, two cases for modelling the bond behaviour between reinforcement and the surrounding concrete were considered. The first case was a rigid model where full bond was assumed between reinforcement and concrete. The second case had a translator element connecting the reinforcement and the surrounding concrete which simulated the bond behavior.

The cracking load obtained from the numerical analysis using ABAQUS was 5.69 kN which was 7.97% higher than the experimental value. Similarly, the ultimate load provided from the numerical analysis was 14.49 kN which was 4.17% lower than the ultimate load reported from the experimental study. Fig. 12 describes the stresses of concrete. The stress of stirrups in the joint reached the yield stress as shown in Fig. 13, therefore the failure mode was joint shear failure due to diagonal tension which coincided with the experimental results. Fig. 14 shows the shape of concrete damage in tension and compression. Plastic strain, shown in Fig. 15, indicates the state and direction of concrete cracks that developed in the numerical model which agrees with the experimental results.

### III. PARAMETRIC STUDY

#### 1.7. Study program

A parametric study involving 30 exterior beam column joints was conducted in this research using the finite element package

Table 3 Numerical analysis results.

Joint No.	Strength (kN)	capacityDeformation capacity (mm)	Joint No.	Strength (kN)	capacityDeformation capacity (mm)
S1	19.90	23.15	S16	19.03	25.02
S2	21.75	21.23	S17	19.27	23.37
S3	24.82	22.58	S18	19.41	23.57
S4	16.27	28.45	S19	19.42	26.88
S5	16.62	24.51	S20	19.64	24.64
S6	17.37	26.15	S21	20.51	24.79
S7	17.61	26.93	S22	19.21	22.11
S8	18.02	25.23	S23	19.981	22.15
S9	18.16	26.05	S24	19.983	22.21
S10	17.87	26.13	S25	19.95	24.20
S11	18.58	25.47	S26	20.73	22.94
S12	18.64	25.86	S27	20.74	23.05
S13	18.28	24.87	S28	20.60	24.38
S14	18.46	22.63	S29	21.43	23.51
S15	18.58	23.89	S30	21.47	23.56

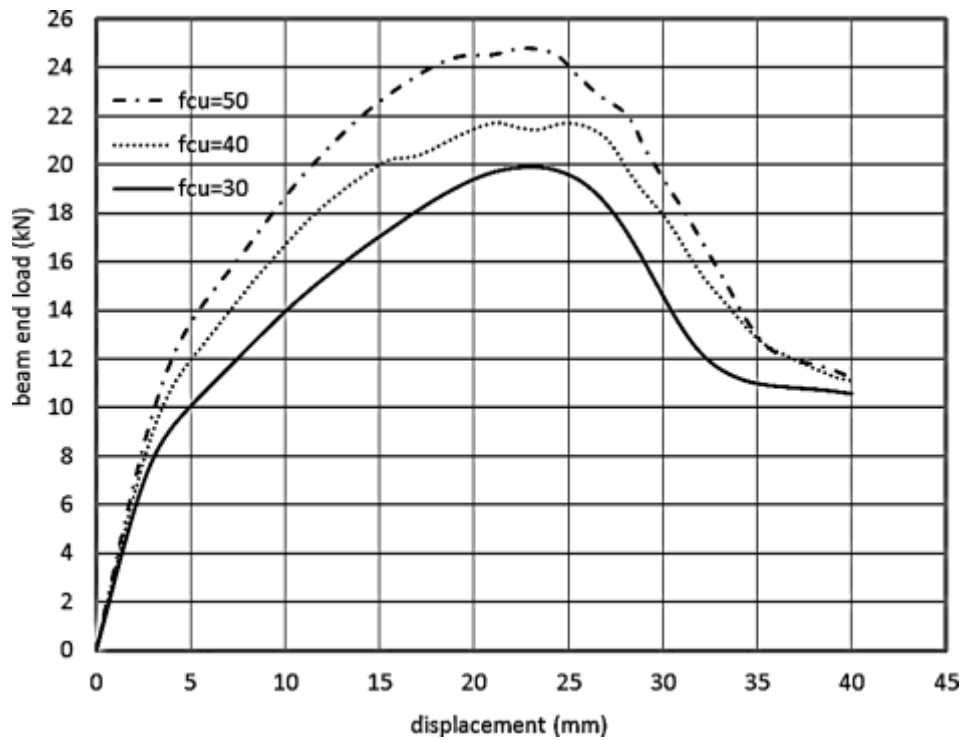


Fig.17 Load-displacement curve for S1,S2, and S3.

ABAQUS and the numerical model described above. The considered parameters were the concrete compressive strength, the column axial load ratio, the number of column stirrups within the joint area and the shape of the beam top reinforcement embedment inside the column. The considered values for concrete compressive strength ( $f_c^d$ ) were 30 MPa, 40 MPa and 50 MPa. Three values for the column axial load ratio ( $P/f_c^d A_c$ ) were considered; 0, 0.3 and 0.6, where  $P$  is the column axial load,  $f_c^d$  is the concrete cylinder compressive strength, and  $A_c$  is the gross cross sectional area. The considered number of column stirrups within the joint area was 2, 3 and 4 stirrups. Straight, L-shaped and U-shaped bars were considered for the embedment shape of top beam reinforcement inside the column and named Type1, Type2 and Type3 respectively. The considered parameters are summarized in Table 2. The concrete dimensions and reinforcement values for the beam and column were taken similar to the values considered by Haach et al. (2014) [12]. Fig. 16 shows the reinforcement details and dimensions of the specimens with two stirrups within the joint.

1.8. Results and discussion

The results of the ultimate loads and deformation capacity according to the conducted numerical analyses are shown in Table 3. The failure of all models considered in the parametric study was due to shear diagonal tension within the joint region. The effect of concrete strength on ultimate load is depicted in Fig. 17 which shows the load-displacement curves for models S1, S2 and S3. All three models had an axial load ratio of 0.3, three column stirrups within the joint and L-shaped beam top reinforcement. The figure shows that increasing the concrete strength lead to an increase in ultimate load. Fig. 18 shows the relation between the concrete strength and the ultimate load. As the concrete strength increased by 67%, from 30 MPa to 50 MPa, the ultimate load increased by 29%, from 19.27 kN to 24.82 kN. It could be observed that nonlinear relation existed between the concrete strength and the ultimate load which agrees with the typically nonlinear relation between the concrete shear and compressive strengths. Additionally, the difference between the ultimate load and concrete strength increase ratios might be attributed to the fact that the joint shear strength was only partially dependent on the concrete strength as the column stirrups also had a consid-

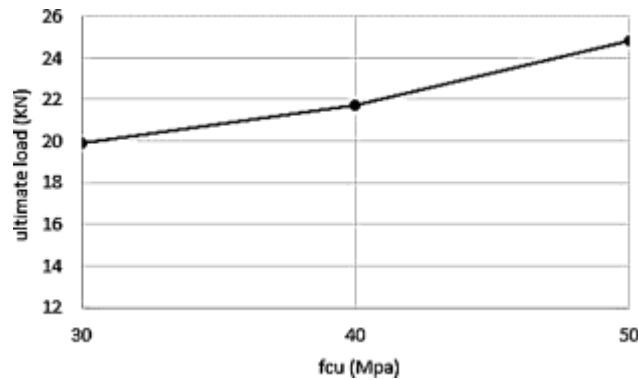


Fig. 18 Effect of concrete compressive strength (no. of stirrups = 3, axial load ratio = 0.3, Type 2).

erable contribution. Table 3 and Fig. 17 also show that the beam tip displacement was reduced as the concrete strength was increased. This might be attributed to the increase in concrete modulus of elasticity typically associated with the increase of concrete strength which resulted in a generally stiffer model. The deformation capacity at the ultimate load

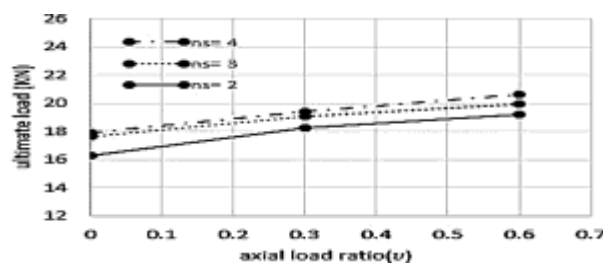


Fig.19 Effect of axial load ratio (Type1).

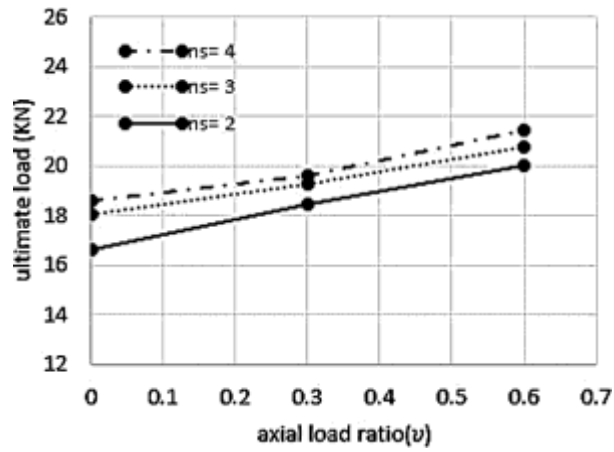


Fig.20 Effect of axial load ratio (Type 2).

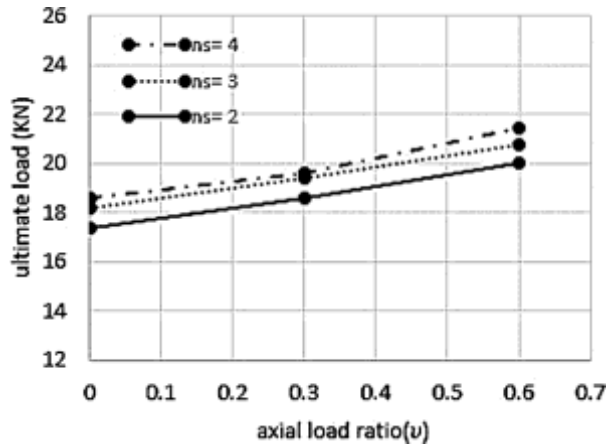


Fig.21 Effect of axial load ratio (Type 3).

decreased by 2.5% as the concrete strength was increased by 67%, despite the increase of the ultimate load by 24.7%.

The effect of the column axial load ratio is shown in Figs. 19–21 for beam top reinforcement shapes Type 1, Type 2 and Type 3, respectively. Each of the three figures shows the

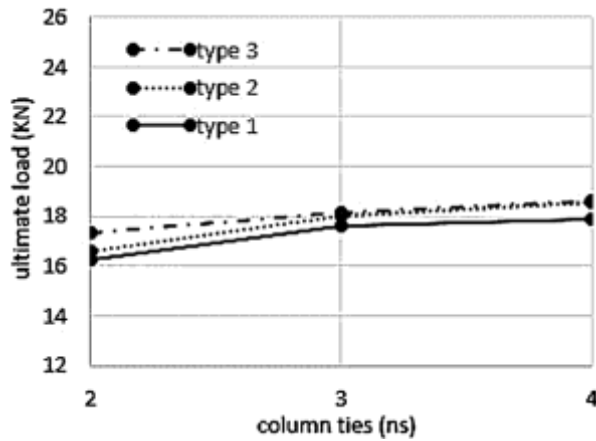
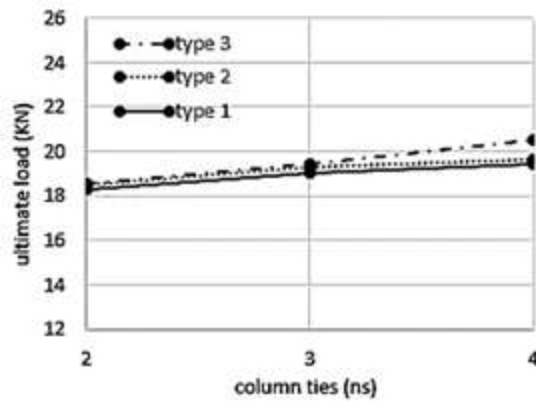
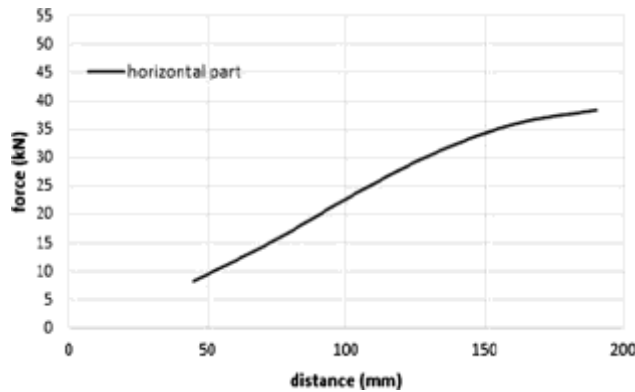


Fig.22 Effect of column stirrups (Axial Load Ratio = 0).



**Fig.23** Effect of column stirrups (Axial Load Ratio = 0.3).

relation between the ultimate load and the column axial load ratio for the different cases of column stirrups numbers. It could generally be observed that increasing the column axial load resulted in an increase of the ultimate load. Applying axial load at the column top increased the ultimate load by average values of 8.48% and 15.67% for column axial load ratios of 0.3 and 0.6 respectively, compared with the corresponding cases without such load. The favorable effect of the column axial load could be attributed to reducing the tensile principal stresses due to joint shear. Figs. 22–24 show the effect of column stirrups on the ultimate load for models with column axial load ratios of 0.0, 0.3 and 0.6, respectively. It could be observed that increasing



**Fig.25** Distribution of steel force for Type 1.

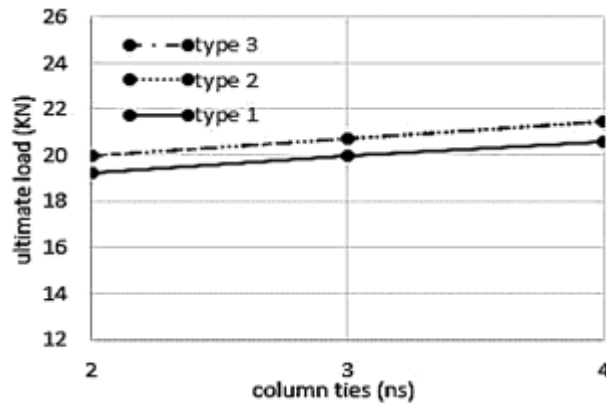
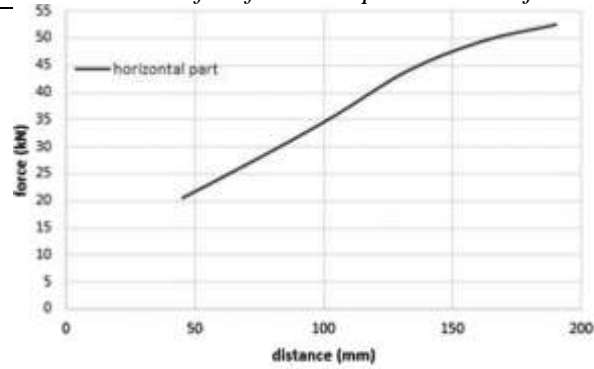
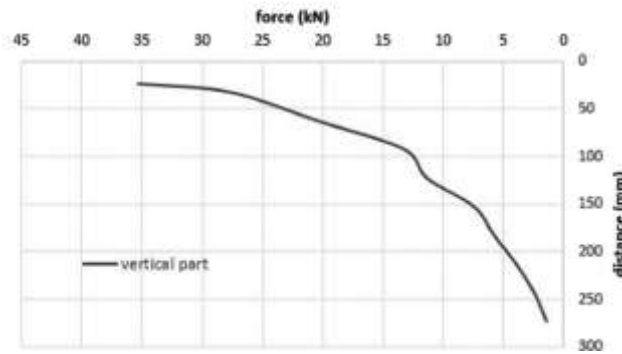


**Fig.24** Effect of column STIRRUPS (Axial Load Ratio = 0.6).



(a) Horizontal Part



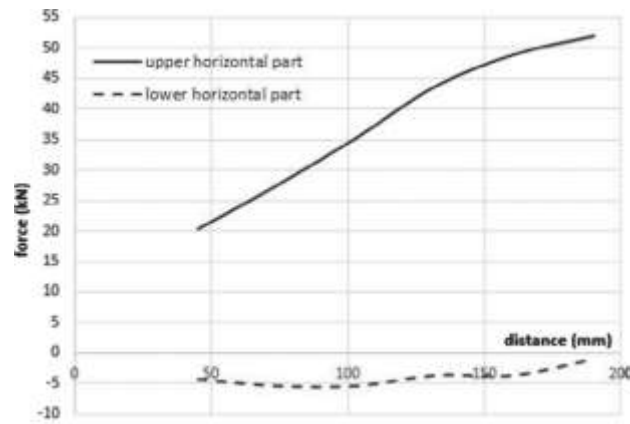
(b) Vertical Part

**Fig.26** Distribution of steel force for Type 2.

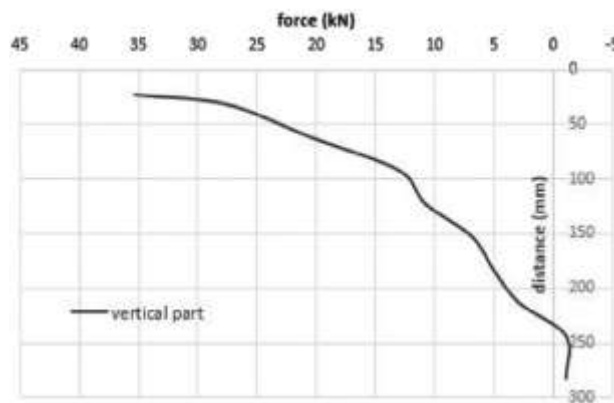
the number of column stirrups within the joint region favorably affected the ultimate load. Increasing the number of column stirrups to 3 and 4 resulted in increasing the ultimate load by average values of 4.92% and 8.08%, respectively, compared with the corresponding cases of two column stirrups.

The shape of the beam top reinforcement also affected the ultimate load of the considered models as shown in Figs. 22–24 as well. The use of straight bars (Type 1) resulted in the least ultimate loads compared with L- (Type 2) and U- (Type 3) shaped bars. This could be attributed to the additional confining effect produced by the L- and U-shaped bars in addition to their contribution in resisting shear cracks in the joint region. The use of L- and U-shaped bars produced similar results as far as the ultimate load and deformation capacity were concerned. In average, the ultimate load was increased by 2.68% and 3.96% for models with L- and U-shaped bars respectively, compared with corresponding models with straight bars.

Figs. 25–27 show an example of the distribution of steel force in the beam top reinforcement in the joint region at failure for Type 1, Type 2 and Type 3, respectively. This force distribution is shown for models S13, S14 and S15 with concrete cylinder strength of 30 Mpa, axial load ratio of 0.3 and two joint stirrups. The tensile force in the top bar for Type 1 almost diminished at the end of the bar while, for Type 2, a considerable portion of the force existed at the end of the horizontal part and transmitted to the vertical part. The top bar tensile force in Type 3 was almost similar to that of Type 2 for both



(a) Horizontal Part



(b) Vertical Part

**Fig.27** Distribution of steel force for Type 3.

the top horizontal part and the vertical part. No tensile force was transmitted to the lower horizontal part. This indicated that the L-shaped (Type 2) bars had an effective and beneficial contribution to the reinforcement anchorage compared with the straight bars. The U-shaped (Type 3) bars had an insignificant effect on the top reinforcement anchorage.

#### IV. CONCLUSIONS

A numerical investigation was performed to study the behavior of exterior reinforced concrete beam column joints subjected to monotonic loading. Thirty numerical models were analyzed using the finite element package ABAQUS to evaluate the effect of concrete strength, column axial load, joint stirrups and shape of beam top reinforcement on the joint ultimate load and deformation capacity. Based on the results of the conducted parametric study, the following conclusions could be made:

- 1) Increasing the concrete strength from 30 MPa to 50 MPa resulted in increasing the beam tip ultimate load by 24.7% and decreasing the deformation capacity at the ultimate load by 2.5%.
- 2) For the studied joints, where the joint failure was due to shear diagonal tension, increasing the column axial load resulted in increasing the beam tip ultimate load. Average ultimate load increase values of 8.48% and 15.67% were obtained for column axial load ratios of 0.3 and 0.6, respectively, compared with the corresponding cases of unloaded columns.
- 3) Increasing the column stirrups within the joint region favorably affected the beam tip ultimate load. Increasing the number of column stirrups to 3 and 4 resulted in increasing the ultimate load by average values of 4.92% and 8.08%, respectively, compared with the corresponding cases of two column stirrups.
- 4) The use of straight bars for beam top reinforcement resulted in generally lower ultimate loads than those obtained with L- and U-shaped bars. Similar joint behavior was demonstrated for the cases of using L- and U-shaped beam top reinforcement.



**REFERENCES**

- [1] R.H.Scott, The effects of detailing on reinforced concrete beam-column connection behaviour, *Struct. Eng.* 70 (18) (1992) 318–324.
- [2] D.E. Parker, P.J.M. Bullman, Shear strength within reinforced concrete beam-column joints, *Struct. Eng.* 75(4)(1997)53–57.
- [3] P.S. Baglin, R.H. Scott, Finite element modeling of reinforced concrete beam-column connections, *ACI Struct. J.* 97(6)(2000)886–894.
- [4] S.J. Hamil, Reinforced Concrete Beam-Column Connection Behavior PhD thesis, University of Durham, England, 2000, pp.34–51.
- [5] P.G. Bakir, M.H. Boduroglu, A new design equation for predicting the shear strength of monotonically loaded exterior beam-column joints, *Eng. Struct. J.* 24 (8) (2002)1105–1117.
- [6] A.E. Atta, S.E. Taher, A.H. Khalil, S.E. El-Metwally, Behaviour of reinforced high-strength concrete beam-column joint. part II: numerical simulation, *Struct. Concr.* 5 (3) (2004)101–112.
- [7] J. Hegger, A. Sherif, W. Roeser, Nonlinear finite element analysis of reinforced concrete beam-column connections, *ACI Struct. J.* 101 (5) (2004)604–614.
- [8] V.G.Haach, Theoretical-Experimental Analysis of the Influence of Normal Force on the Exterior Reinforced Concrete Joints, MSc thesis. Sao Carlos (Brazil): University of São Paulo, São Carlos Engineering School, 2005, pp. 159 (in Portuguese).
- [9] S.S. Patil, S.S. Manekari, Analysis of reinforced beam-column joint subjected to monotonic loading, *Int. J. Eng. Innovat. Technol. (IJEIT)* 2 (10) (2013)149–158.
- [10] S.V. Chaudhari, K.A. Mukane, M.A. Chakrabarti, Comparative study on exterior RCC beam column joint subjected to monotonic loading, *Int. J. Comput. Appl.* 102 (3)(2014) 34–39.
- [11] T.M. Tran, M.N. Hadi, Shear strength model of reinforced-concrete exterior joint under cyclic loading, *Struct. Build.* 170(8)(2017)603–617.
- [12] V.G. Haach, A.L. El Debs, M.Kh El Debs, Influence of High column axial loads in exterior R/C beam-column joints, *KSCEJ. Civ. Eng.* 18 (2) (2014)558–565.
- [13] ABAQUS/CAE User's Manual Version 6.13. 2013. Simulia.
- [14] CEB-FIP Model Code, Design Code, Committee Euro- International du Beton, Lausanne, Thomas Telford Services Ltd., London, 1990.